

## Controlling the Extent of Diradical Character by Utilizing Neighboring Group Interactions

Yousung Jung and Martin Head-Gordon\*

Department of Chemistry, University of California at Berkeley, and Chemical Sciences Division, Lawrence Berkeley National Laboratory, Berkeley, California 94720

Received: February 24, 2003; In Final Form: May 23, 2003

The extent of diradical character of a recently reported “localized singlet diradical that is indefinitely stable at room temperature” ( $R_4P_2B_2R'_2$ ) is assessed by electronic structure calculation of orbital occupation numbers compared to other well-studied diradicaloid systems. Our study shows that it has significantly less diradical character (and much more bonding character) than other typical organic diradicals. How this molecule,  $R_4P_2B_2R'_2$ , attains this stability (bonding character) despite the long (2.60 Å) B–B distance is satisfactorily explained using a simplified model compound,  $H_4P_2B_2H_2$ , and frontier orbital mixing ideas. Increasing bond length usually makes a molecule more diradicaloid. For example, as the H–H bond stretches in a homolytic single-bond breaking process,  $H_2$  becomes more and more diradical-like, eventually becoming a pure diradical at complete separation. A counter-example is presented in this paper in which the molecule with a longer B–B “bond” distance (2.60 Å),  $H_4P_2B_2H_2$ , represents less diradical character than the molecule with a shorter B–B distance (2.04 Å),  $H_4N_2B_2H_2$ . This novel observation is also explained in terms of molecular orbital mixing and second-order perturbation theory. Electronic structure calculations reveal that the coupling of radical centers to the adjacent groups via through-bond interaction, as well as the distance between the two radical centers, is critical in determining the extent of diradical character.

## Introduction

Diradicals are molecules with two unpaired electrons occupying two degenerate or nearly degenerate molecular orbitals (MO), i.e., two singly occupied MO's. These two unpaired electrons can interact with each other to form either a singlet spin state (antiferromagnetic coupling) or a triplet (ferromagnetic coupling) depending upon the nature of spin coupling.<sup>1</sup> The understanding of spin interaction in diradicals can serve as a basis for making high spin organic molecules and can be further utilized in developing new organic materials with magnetic properties using those high spin polyradicals as a building block.<sup>1b,14c</sup>

Spintronics (spin-based electronics) is another area in which the control of electron spin and its interaction with magnetic materials are critical for the success of devices.<sup>15</sup> Contrary to conventional electronics that uses electron charge as a carrier of information, spintronics uses electron spin for encoding information. New devices that can utilize the electron spin degree of freedom could have various advantages compared to conventional charge-based devices, such as increased data processing speed, decreased electric power consumption, etc. Therefore, there is a significant need for better understanding of spin interactions (and possibly the ability to control spins freely).

Diradicals, however, are very short-lived under standard laboratory conditions. Although a wide variety of chemical reactions involve (or are predicted to involve) diradicals as reaction intermediates,<sup>2</sup> their short lifetimes make experimental studies still difficult.<sup>2</sup> In general, the triplet diradical states are *relatively* more stable than the singlet states when the MOs associated with diradical character are (nearly) degenerate and orthogonal, according to Hund's rule. However, of course,

depending upon the strength of exchange interaction between the two radical electrons and overall electron correlations in the system, Hund's rule can also be violated and singlet ground-state diradicals can exist.<sup>2a–c</sup> Very short lifetimes of singlet diradicals are manifestations of the fact that singlet diradicals are usually not energy minima on chemical reaction coordinates. Triplet diradicals appearing during reaction, on the other hand, are usually energy minima and true intermediates, thus having a *relatively* longer lifetimes compared to singlet states.

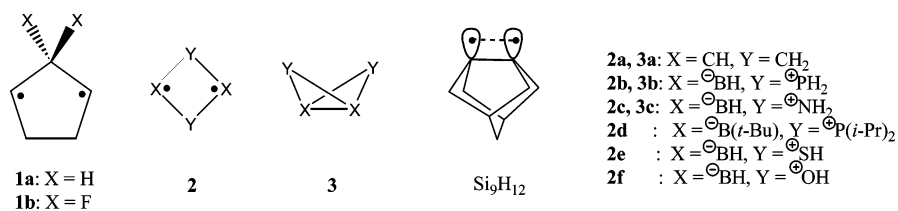
Many localized hydrocarbon diradicals have been synthesized and characterized<sup>3</sup> ever since the complete characterization of 1,3-cyclopentanediyli, **1a** (Scheme 1), both experimentally<sup>4</sup> and theoretically.<sup>5</sup> **1a** has a triplet ground state, lying about 1 kcal/mol below the singlet state in accord with Hund's rule. However, most chemical reactions occur on singlet potential energy surfaces, where triplet intermediates are spin-forbidden.<sup>6</sup> Also, triplet diradicals are relatively well understood due to their comparatively longer lifetimes compared to singlet diradicals. Therefore, both theoretical and experimental efforts have been directed toward preparation of stable singlet diradicals.<sup>7</sup>

One of the more stable singlet diradicals is **1b**, which has been experimentally confirmed to have a singlet ground state, as a result of fluorine substitution.<sup>7</sup> Further substituent changes have increased the lifetime to microseconds.<sup>7c</sup> The tuning of singlet–triplet energy separation by structural variations has also been studied to control the spin state of diradicals.<sup>7f–h</sup>

Recently, a new “localized singlet diradical (**2d**) that is indefinitely stable at room temperature” was reported using non-carbon-based skeleton.<sup>8</sup> On the basis of <sup>11</sup>B and <sup>31</sup>P NMR chemical shifts, a long B–B distance (2.57 Å) and perfectly planar PBPB four-membered ring geometry from X-ray diffraction, together with silent electron paramagnetic resonance signal (for spin state), the authors classified it as a singlet localized diradical. We present in this paper a different

\* Corresponding author. E-mail: mhg@bastille.cchem.berkeley.edu.

## SCHEME 1: Diradicaloid Systems under Consideration in This Work



perspective on this molecule (and some related compounds) from a theoretical point of view.

Attempts to determine the extent of singlet diradical character have been made using a modified one particle density matrix<sup>18a</sup> and the magnitude of  $\langle S^2 \rangle$  using a broken symmetry spin-unrestricted density functional theory (UDFT).<sup>18b</sup> The main computational measure of diradical character we will use in this paper is the relative value of the occupation numbers for bonding and antibonding orbitals associated with the two radical sites, as introduced long ago.<sup>1c–e</sup> These orbital occupation numbers are closely related to the one particle density matrix that Staroverov and Davidson used to quantify the extent of diradical character.<sup>18a,c</sup> The more closely bonding and antibonding occupation numbers approach each other, the closer the system is to a pure diradical. For instance, dissociated singlet H<sub>2</sub> has HOMO (highest occupied molecular orbital) and LUMO (lowest unoccupied molecular orbital) occupation numbers of 1 each, whereas H<sub>2</sub> at equilibrium has natural orbital occupation numbers<sup>16</sup> of about 1.98 and 0.02 with the 6-311++G(d,p) basis.

To employ this measure of diradical character requires that multiconfigurational wave functions be used.<sup>17</sup> Methods that employ single configuration wave functions, like restricted Hartree–Fock (RHF) theory and density functional theory (DFT), yield occupation numbers that are either exactly 0 or exactly 2, and are thus inappropriate. The simplest multireference method that can describe the bonding and antibonding occupation numbers in a balanced way is the perfect-pairing (PP) method.<sup>9a–c</sup> In the PP method (equivalent to the generalized valence bond perfect pairing method) each electron pair is described by a bonding and an antibonding orbital, which are optimized, along with their occupation numbers.

It should be noted that defining what is a “pure” diradical is practically not possible in an absolute sense, because most organic diradicals indeed have LUMO occupation numbers less than (but close to) 1, and in some cases, they are even around 0.6 (**1b**). In other words, there is no sharp cutoff to determine whether a molecule is a diradical or not based only on the LUMO occupation number. Thus, our intention of using LUMO occupation numbers as an indication of the extent of diradical character is as a *scale* on which different molecules (e.g., a recently reported diradical, **2d**, and other diradicaloid systems that are already well understood) can be compared. We will examine various 4- and five-membered ring diradicals **1a**, **1b**, and **2a** (Scheme 1). A Si<sub>9</sub>H<sub>12</sub> cluster was also selected for comparison, because the Si(100) surface is another stable diradicaloid system, at least in UHV.<sup>12,13</sup> The top two silicon atoms in Si<sub>9</sub>H<sub>12</sub> dimerize to form a strong  $\sigma$  bond and a weaker  $\pi$  bond. Due to the small HOMO–LUMO gap, this weak  $\pi$  bond attains a fairly large amount of diradical character. Si<sub>9</sub>H<sub>12</sub> is the smallest surface cluster model for the reconstructed Si(100) surface.

One of the generally accepted concepts regarding diradicals is that increasing bond length makes the molecule more diradicaloid. Akin to a homolytic single bond dissociation, as

the bond length increases, the molecule becomes more and more open-shell-like and finally has two singly occupied orbitals at infinite separation, namely, becoming a pure diradical. The dissociation of H<sub>2</sub> is the simplest example. However, we report in this paper a counter-example in which the molecule with a longer B–B “bond” distance, **2b**, is less diradicaloid than the one with a shorter B–B distance, **2c**. This novel observation is understood with the help of orbital mixing and second-order perturbation theory.

We note that similar calculations on **2b**, **2d** and some variants of **2d** were recently reported elsewhere.<sup>20</sup> The extent of diradical character was assessed using LUMO occupation numbers, and possible substituents for future synthesis of **2d** moieties that are more diradicaloid were suggested. The LUMO occupation numbers for **2b** and **2d** were calculated to be 0.21 and 0.19, which are similar to those we report here. Substitution with the more electropositive SiMe<sub>3</sub> instead of *i*-Pr as a phosphorus substituent in **2d** increased the LUMO occupation number to 0.30.<sup>20a</sup>

This paper will mainly focus on the following two points that are new from ref 20. (1) How is diradicaloid **2d** compared to other well-studied diradical systems, and can a singlet diradical exist with indefinite stability at room temperature without losing significant diradical character at the same time? (2) How is it possible that the molecule with a shorter bond distance represents more diradical character than the molecule with a longer distance, unlike usual diradical systems? This question will be addressed by comparative frontier orbital analysis on **2d** and related compounds.

## Theoretical Methods

The coupled cluster (CC) formulation of PP<sup>9a–c</sup> was used with the 6-31G(d) basis,<sup>9d</sup> namely CC-PP/6-31G(d), in a development version of the Q-Chem program.<sup>9e</sup> The active space for the PP calculations was chosen such that one “occupied” and one (correlating) “virtual” orbital are associated with each pair of valence electrons. For example, 22 active orbitals (5 from phosphorus, 3 from boron, and 1 from hydrogen) were used for **2b** (H<sub>4</sub>P<sub>2</sub>B<sub>2</sub>H<sub>2</sub>). All geometric parameters and orbital occupation numbers reported here are at the optimized geometries within a given symmetry (flat or bent) at the CC-PP/6-31G(d) level of theory. However, because **2d** was too big a system to tractably perform a full valence PP geometry optimization at present, it was instead optimized with UB3LYP/6-31G(d), spin-unrestricted density functional theory. Subsequently, a single point CC-PP/6-31G(d) calculation was performed on the UB3LYP/6-31G(d) optimized geometry to get occupation numbers.

Our CC-PP code is at present restricted to singlet states, and thus, to obtain singlet–triplet gaps, we had to use another method. Standard Kohn–Sham DFT may be unreliable because of the significant nondynamical correlation effects found in singlet diradicals. Instead, singlet–triplet energy splittings for the various diradicals were calculated using a recently developed spin-flip time-dependent density functional theory with a

Tamm–Dancoff approximation (SF-TDDFT/TDA)<sup>11d</sup> with the 6-31G(d) basis. In the spin-flip (SF) model,<sup>11a–d</sup> closed and open shell singlet states as well as an  $M_s = 0$  triplet state are described by excitations from an  $M_s = 1$  triplet state as a reference state. In the SF-TDDFT/TDA method, dynamical correlation is recovered through the time-dependent density functional theory (TDDFT) combined with the Tamm–Dancoff approximation (TDA),<sup>11e–g</sup> and nondynamical correlation is recovered by the spin-flip excitation part (SF). Full details as well as application to twisted ethylene and several other diradical systems can be found in ref 11. Following ref 11d, we used SF-TDDFT/TDA with a 50/50 functional (50% Hartree–Fock + 8% Slater + 42% Becke for exchange functional, and 19% VWN + 81% LYP for correlation functional). In ref 11d, this gives the best singlet–triplet splittings compared to experiments. Energies reported (and cited) in this paper are electronic energies without zero point energy correction.

Though PP orbitals are the simplest qualitatively correct orbitals that can be uniquely defined for a pair of bonding and antibonding orbitals, particularly for diradicaloid systems, associating orbital energies with PP orbitals appear to be somewhat inconsistent. This is because PP orbitals are part of the 2-electron pair function in PP theory whereas the Fock operator used to obtain orbital energies is a one-particle operator. We avoid this difficulty by choosing to use DFT calculations at the B3LYP/6-31G(d) level, in which orbital energies are well defined with the Kohn–Sham orbitals and the Fock operator, for estimating orbital energies.

For highly diradicaloid systems such  $^{\ominus}\text{BH}_2^- - ^{\ominus}\text{BH}_2^*$  at a long B–B distance (used for estimating initial bonding–antibonding gap in this work),<sup>24</sup> bonding and antibonding orbitals are virtually degenerate and the spin-unrestricted method will most likely result in two localized orbitals, one ( $\alpha$  electron) on one radical site and the other ( $\beta$  electron) on the other radical site. The same situation occurs in the dissociation limit of  $\text{H}_2$  using the unrestricted method, in which the highest occupied molecular orbitals in  $\alpha$  and  $\beta$  spaces are 1s orbitals localized on each hydrogen atom, respectively. In other words, unrestricted (localized) orbitals will not have the physical character of bonding and antibonding combinations of the two radical orbitals. This makes the use of spin-unrestricted DFT somewhat inappropriate for this *particular purpose*. Therefore, we use *spin-restricted* DFT, namely, RB3LYP/6-31G(d), for estimating orbital energies for orbital interaction diagrams. However, we note that RDFT solutions for  $^{\ominus}\text{BH}_2^- - ^{\ominus}\text{BH}_2^*$  species with large B–B distances are unstable toward spin symmetry breaking in the orbital space because they have substantial diradical character, as shown by computing and diagonalizing the second derivative of energy with respect to orbital rotations.<sup>22</sup>

Last, the magnitude of the expectation value  $\langle S^2 \rangle_{\text{UB3LYP}}$  was calculated using broken symmetry spin-unrestricted DFT (UB3LYP/6-31G(d)) calculations at the PP optimized geometries. In fact, the Slater single determinant of Kohn–Sham (KS) orbitals that produces the density is clearly not the correct wave function, which makes the use of this DFT “wave function” to calculate  $\langle S^2 \rangle$  not theoretically rigorous. Because of this problem, spin contamination in DFT is not as meaningful as in HF theory.<sup>19</sup> Empirically, however,  $\langle S^2 \rangle$  calculated from KS orbitals has been used for estimating the extent of diradical character.<sup>18b</sup> Therefore, we also report  $\langle S^2 \rangle$  values for various diradicaloid compounds using UB3LYP.

## Results and Discussion

**Quantification of Diradical Character.** The parent molecule, **2b**, for the actual “diradical”, **2d**, is topologically

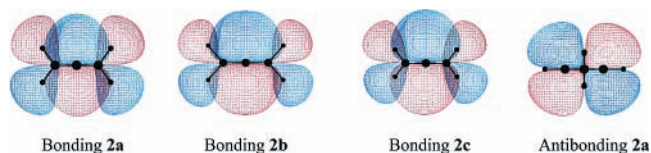


**Figure 1.** HOMO (bonding) and LUMO (antibonding) radical orbitals of **2a**, **2b**, and **2c**. A fixed percentage (90%) of electron density containment was used for drawing the orbitals to scale them equally. To show the antibonding character of the LUMO between the two  $\text{B}(p_z)$  orbitals more clearly, a geometry rotated  $90^\circ$  with respect to the  $z$ -axis compared to the corresponding bonding orbital was used. Antibonding orbitals for **2b** and **2c** look essentially the same as that of **2a**, and are thus omitted here.

**TABLE 1: Bonding (HOMO) and Antibonding (LUMO) Occupation Numbers of Various Diradicaloid Molecules**

	bonding occupation	antibonding occupation	$\langle S^2 \rangle_{\text{UB3LYP}}$
<b>1a</b>	1.073	0.927	1.001
<b>1b</b>	1.417	0.583	0.805
<b>2a</b>	1.140	0.860	1.004
<b>2b</b>	1.779	0.221	0.009
<b>2c</b>	1.563	0.437	0.730
<b>2d</b>	1.831	0.169	0.002
<b>2e</b>	1.684	0.316	0.009
<b>2f</b>	1.467	0.533	0.794
$\text{Si}_9\text{H}_{12}$	1.682	0.318	0.167 <sup>a</sup>

<sup>a</sup> The existence of a spin symmetry broken solution for  $\text{Si}_9\text{H}_{12}$  will be presented in more detail elsewhere.<sup>21</sup>

**TABLE 2: Comparison of **2a**, **2b**, and **2c** in Terms of Geometric Parameters and Other Important Properties**

	X–X (Å)	X–Y (Å)	LUMO occupation	$\Delta E_{\text{rel}}$ (kcal/mol) <sup>a</sup>	$\Delta E_{\text{ST}}$ (kcal/mol) <sup>b</sup>
<b>2a</b> (flat)	2.088	1.524	0.860	40.9	2.3
<b>3a</b> (bent)	1.489	1.513	0.018		
<b>2b</b>	2.602	1.915	0.221	10.2	–27.3 <sup>c</sup>
<b>3b</b>	1.849	1.918	0.017		
<b>2c</b>	2.038	1.580	0.437	44.7	–13.1
<b>3c</b>	1.612	1.618	0.022		

<sup>a</sup>  $\Delta E_{\text{rel}} = E_{\text{flat}}(2) - E_{\text{bent}}(3)$  at the CC–PP/6-31G(d) optimized geometries. <sup>b</sup>  $\Delta E_{\text{ST}} (=E_{\text{singlet}} - E_{\text{triplet}})$  is an adiabatic gap using SF-TDDFT/TDA with the 6-31G(d) basis (ref 11). <sup>c</sup> See ref 11h.

equivalent to **2a**. **2a** is a transition structure on a singlet potential energy surface<sup>10</sup> with a triplet ground state ( $\Delta E_{\text{ST}} = 2.3$  kcal/mol). Figure 1 depicts the HOMO and LUMO of **2a**, **2b**, and **2c**, and their occupation numbers are summarized in Table 1. Table 1 also includes occupation numbers of related diradicaloid systems. Table 2 compares various geometric parameters and properties of **2a**, **2b**, and **2c**. At flat geometries, the LUMO occupation number for **2a** is 0.860 but only 0.221 for **2b**. This means that the HOMO–LUMO gap in **2b** must be relatively large compared to **2a**.

The comparison of **2b** with a  $\text{Si}_9\text{H}_{12}$  dimer further suggests that the HOMO–LUMO gap in **2b** is larger than that in a  $\text{Si}_9\text{H}_{12}$  dimer. The LUMO occupation number of  $\text{Si}_9\text{H}_{12}$  is 0.318 due to a weak  $\pi$  bonding character (or small HOMO–LUMO gap), as can be seen in Table 1. Clearly, **2b** is less diradicaloid than the silicon dimer. In addition, the synthesized molecule **2d** has an even smaller LUMO occupation number of 0.169, meaning that **2d** has less diradical character than **2b** or  $\text{Si}_9\text{H}_{12}$ . As one would expect, however, as the geometries of **2a** and **2b** transform to the bent structures, **3**, they slowly start forming  $\sigma$  bonds between X’s. Eventually, the molecules become “completely” closed shell, and the LUMO occupation numbers approach zero, as shown in Table 2.

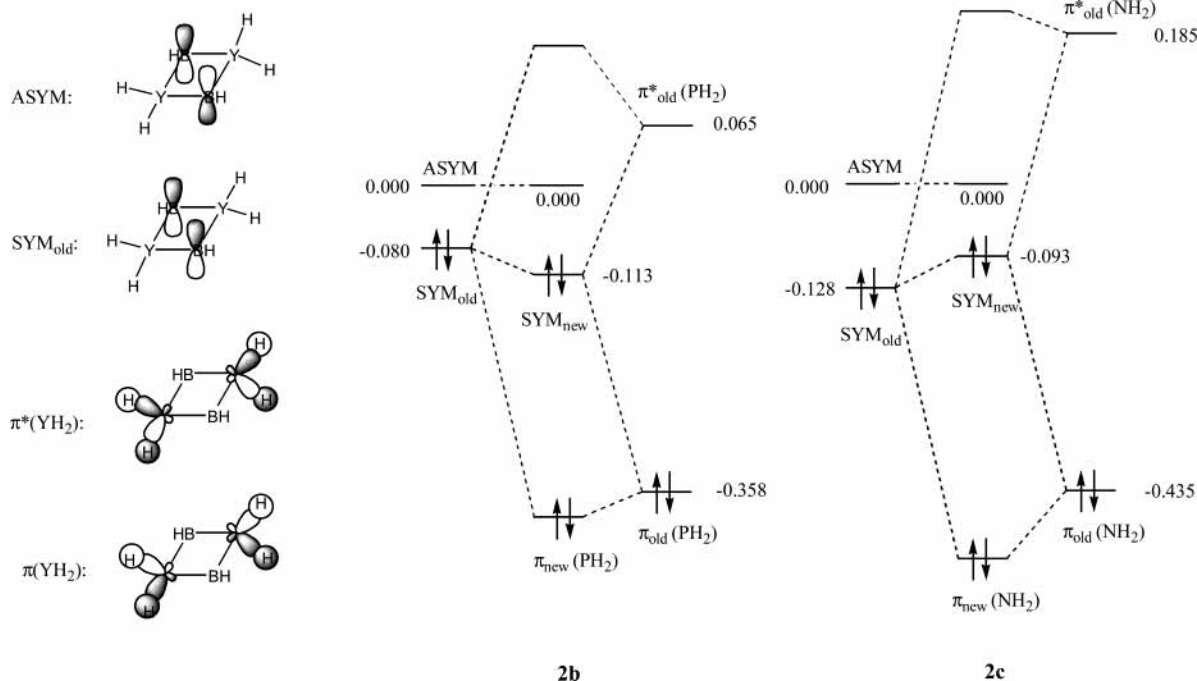


**Figure 2.** Orbital interaction diagram for **2b** and **2c**. The diradical bonding MO ( $\text{SYM}_{\text{old}}$ ) couples to the bonding or antibonding MO ( $\pi_{\text{old}}$  or  $\pi^*_{\text{old}}$ ) of the adjacent groups with the same symmetry. For **2b**,  $\text{SYM}_{\text{old}}$  mixes more strongly with  $\pi^*_{\text{old}}$  than with  $\pi_{\text{old}}$ , whereas, for **2c**, mixing with  $\pi_{\text{old}}$  is stronger than with  $\pi^*_{\text{old}}$ . Orbital energies are given in atomic units (1 au = 27.21 eV).

The stabilizing energies ( $\Delta E_{\text{rel}}$ ) toward the bent structures are 40.9 and 10.2 kcal/mol for **2a** and **2b**, respectively. The small  $\Delta E_{\text{rel}}$  for **2b** implies that **2b** is thermodynamically already a relatively stable species, presumably because it possesses a relatively small degree of diradical character. The singlet–triplet energy gaps ( $\Delta E_{\text{ST}}$ ) are calculated to be +2.3 and –27.3 kcal/mol for **2a** and **2b**, respectively, with the positive sign meaning that the triplet is the ground state. **2a** is a ground-state triplet with a small singlet–triplet splitting (2.3 kcal/mol), in accord with Hund’s rule for a nearly degenerate diradical. On the other hand, considering the fact that diradicals usually have a small singlet–triplet gap, –27.3 kcal/mol in **2b** suggests that the extent of diradical character of **2b** is not too large. The actual molecule **2d** has an even larger singlet–triplet gap of –33.7 kcal/mol, implying the same meaning. Consistently, **2d** is predicted to be less diradical-like than the model **2b**.

Next, a PP calculation on **2c**, in which phosphorus is replaced by nitrogen, was performed. The LUMO occupation number in **2c** was calculated to be 0.437, representing much more diradical character than **2b** (0.221). The smaller singlet–triplet gap (–13.1 kcal/mol) in **2c** than in **2b** (–27.3 kcal/mol) also suggests the same. In contrast, the B–B distance in **2c** was significantly reduced compared to **2b**, from 2.60 to 2.04 Å. This is a striking result because usually increasing bond length makes the molecule more diradicaloid. Although this appears to be a novel observation, it can be satisfactorily explained using standard frontier orbital mixing arguments,<sup>14</sup> which appear in the next section in detail.

Last, it is worthwhile to see the effects of fluorine substitution in **1b**. As Xu et al showed theoretically,<sup>7a</sup> the fluorine substitution in **1b** causes it to have a singlet ground state (6.1 kcal/mol at the ROHF-TCSCF level, and 9.7 kcal/mol at CASPT2N, below the triplet), whereas **1a** has a triplet ground state with a singlet–triplet gap of about 1 kcal/mol with various levels of theory.<sup>5</sup> Clearly, the fluorine substituents stabilized a singlet state over a triplet, which is a violation of Hund’s rule for diradicals. On the other hand, **1a** and **1b** have LUMO occupation numbers of 0.927 and 0.583, respectively, as can be seen in

Table 1. This means that **1b** has less diradical character than **1a** as a result of fluorine substitution. Therefore, although fluorine substitution indeed changed the ground spin state of **1b** (from triplet to singlet), it also changed (reduced) the degree of diradical character of **1b** (from 0.927 to 0.583). In other words, the price to pay for stabilizing singlet diradicals is that, almost by definition, one must remove some diradical character from, and add bonding character, to the system. In this context, we conclude that the reason that **2d** is indefinitely stable in a singlet state is probably due to its dominant bonding character (and moderate extent of diradical character).

Table 1 also shows  $\langle S^2 \rangle_{\text{UB3LYP}}$  for various diradicaloid compounds, in which its overall trend on the extent of diradical character is roughly similar to that obtained from PP occupation numbers. In Table 1, true diradicals **1a** and **2a** have  $\langle S^2 \rangle_{\text{UB3LYP}}$  of slightly more than 1. The fact that they are even slightly greater than 1 suggests that the triplet is slightly dominant over the singlet in this “spin contaminated” state (it would be exactly 1 if singlet and triplet are exactly degenerate). Indeed, this is consistent with the fact that these diradicals **1a** and **2a** have triplet ground states with very small singlet–triplet gaps.<sup>4,5,10</sup> The experimentally observed singlet diradical **1b** has a  $\langle S^2 \rangle_{\text{UB3LYP}}$  somewhat smaller than 1 (0.805), empirically implying reduced diradical character compared to **1a** and **2a**,<sup>18b</sup> as evidenced in the PP LUMO occupation numbers in Table 1. On the other hand, **2b** and **2d** have essentially no spin contamination (or  $\langle S^2 \rangle_{\text{UB3LYP}} \sim 0$ ), implying that they have lost a significant amount of diradical character. Again, this supports our conclusion above based on PP LUMO occupation numbers that **2d** (and **2b**) has only a modest amount of diradical character, and this is the driving force for **2d** to exist with indefinite stability.

**Analysis of Orbital Interactions.** We first briefly summarize the notation used in this paper (Figures 2 and 3).  $\text{SYM}_{\text{old}}$  and  $\text{ASYM}$  are the initial bonding and antibonding combinations of radical orbitals, respectively, before considering any other perturbation, and  $\text{SYM}_{\text{new}}$  is a modified  $\text{SYM}_{\text{old}}$  after considering the orbital interaction ( $\text{ASYM}$  remains unchanged due to the absence of orbital mixing as will be discussed below). The terms

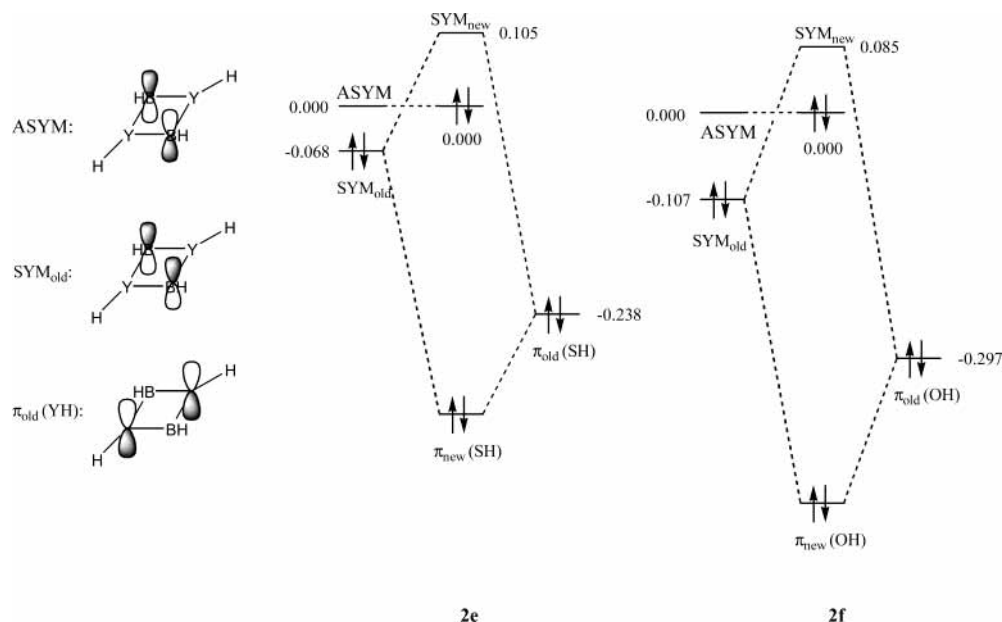


**Figure 3.** Orbital interaction diagram for **2e** and **2f**. The diradical bonding MO ( $\text{SYM}_{\text{old}}$ ) couples to the symmetric combination ( $\pi_{\text{old}}$  (YH)) of atomic  $p_z(\text{Y})$  orbitals of the adjacent groups (SH or OH) with the same symmetry. In both cases, mixing between  $\text{SYM}_{\text{old}}$  and  $\pi_{\text{old}}$  is strong enough to lift  $\text{SYM}_{\text{old}}$  all the way up to above ASYM. As a result, ASYM (the antisymmetric combination of the two radical boron  $p_z(\text{B})$  orbitals) becomes a HOMO (highest occupied molecular orbital) after the orbital interaction.

HOMO and LUMO are used to literally denote the *final* highest occupied and lowest unoccupied molecular orbitals. Therefore, it is possible for ASYM to become HOMO and  $\text{SYM}_{\text{new}}$  to become LUMO as a result of orbital interactions (like in Figure 3), although  $\text{SYM}_{\text{old}}$  is always lower in energy than ASYM from second-order perturbation theory. We use  $\pi_{\text{old}}$  and  $\pi_{\text{old}}^*$  to denote neighboring group orbitals that can mix with  $\text{SYM}_{\text{old}}$ . However, it should be noted that, although we use  $\pi_{\text{old}}$  and  $\pi_{\text{old}}^*$  for distinction, they in fact both have  $\pi$  symmetry, as should be clear from Figure 2.

Orbital interaction diagrams for **2b** and **2c** are summarized in Figure 2.<sup>14</sup> Degenerate atomic  $p_z$  orbitals centered on boron atoms on opposite sides of the ring can interact with each other to form bonding and antibonding MOs, in which a  $\text{SYM}_{\text{old}}$ –ASYM gap is determined by the extent of overlap of two  $p_z(\text{B})$  orbitals from degenerate perturbation theory. In other words, the shorter the B–B distance is, the more overlap occurs, and the larger the  $\text{SYM}_{\text{old}}$ –ASYM gap that is created. Therefore, **2c** (2.04 Å) with a shorter B–B distance has a larger  $\text{SYM}_{\text{old}}$ –ASYM gap than **2b** (2.60 Å) as a result of  $p_z(\text{B})$ – $p_z(\text{B})$  orbital interaction. However, this is before interaction with neighboring group orbitals (hence the designation  $\text{SYM}_{\text{old}}$ ).

One pair of neighboring group bonding and antibonding orbitals ( $\pi_{\text{old}}$  and  $\pi_{\text{old}}^*$  in Figure 2) of **2** have the same symmetry as  $\text{SYM}_{\text{old}}$ , which allows a mixing between them. It is this (through-bond) orbital mixing that causes **2c** to become more diradicaloid with a smaller final  $\text{SYM}_{\text{new}}$ –ASYM gap than **2b**, although **2c** initially had a larger  $\text{SYM}_{\text{old}}$ –ASYM gap than **2b**. As can be seen in Figure 2,  $\pi_{\text{old}}$  mixes with  $\text{SYM}_{\text{old}}$  to lift up the  $\text{SYM}_{\text{old}}$  level (and lower  $\pi_{\text{old}}$  level), whereas  $\pi_{\text{old}}^*$  mixing with  $\text{SYM}_{\text{old}}$  lowers the  $\text{SYM}_{\text{old}}$  level (and lifts up  $\pi_{\text{old}}^*$  level). This mixing is visually evident in the bonding HOMO ( $\text{SYM}_{\text{new}}$ ) shown previously in Figure 1. In contrast, the antibonding LUMO (ASYM) in Figure 1 clearly shows no evidence of orbital mixing as we present in the orbital–orbital interaction diagram in Figure 2.

The relative strength of mixing of  $\text{SYM}_{\text{old}}$  with  $\pi_{\text{old}}$  or  $\pi_{\text{old}}^*$  must determine the final  $\text{SYM}_{\text{new}}$ –ASYM gap, and the degree

of diradical character. In the spirit of second-order perturbation theory, the splitting ( $\Delta$ ) is dictated by the energy gap ( $\delta\epsilon$ ) between the two MOs that are mixing and the matrix elements ( $V$ ) between them, namely  $\Delta \sim V^2/\delta\epsilon$ . Of course, the energy gap  $\delta\epsilon$  between unperturbed orbitals is not obtainable from ordinary electronic structure calculations, because those calculations already include all interactions between them. Accordingly, we instead used model systems to estimate unperturbed orbital energies (or  $\delta\epsilon$ 's). A diradical  ${}^{\ominus}\text{BH}_2$ – ${}^{\ominus}\text{BH}_2^{\bullet}$  (with B–B distances of 2.60 and 2.04 Å as models for **2b** and **2c**, respectively) was used for estimating bonding and antibonding  $\text{SYM}_{\text{old}}$ –ASYM gaps.<sup>24</sup>  $\text{PH}_3$  and  $\text{NH}_3$  were used for orbital energies of  $\pi_{\text{old}}$  (Y) and  $\pi_{\text{old}}^*$  (Y).<sup>23</sup> Orbital energies (in hartrees or atomic units) in Figure 2 are shifted such that the energy of ASYM is always zero. The focus in Figures 2 and 3 should be on the relative orbital energy differences, rather than the absolute values of orbital energies.

In **2b**, the initial  $\text{SYM}_{\text{old}}$ –ASYM gap is 0.080 au and the orbital interaction of  $\text{SYM}_{\text{old}}$  with  $\pi_{\text{old}}$  and  $\pi_{\text{old}}^*$  causes the gap to become 0.113 au. Assuming that  $V$  (the matrix element) between  $\text{SYM}_{\text{old}}$  and  $\pi_{\text{old}}$  and  $V$  between  $\text{SYM}_{\text{old}}$  and  $\pi_{\text{old}}^*$  are about the same (which should be reasonable because  $\pi_{\text{old}}$  and  $\pi_{\text{old}}^*$  are localized on the same atoms and spatially similar),  $\delta\epsilon$  will be the dominant factor determining their relative strength of mixing, within second-order perturbation theory. In **2b**,  $\delta\epsilon$  (0.145 au) of  $\text{SYM}_{\text{old}}$ – $\pi_{\text{old}}^*$  is smaller than  $\delta\epsilon$  (0.278 au) of  $\text{SYM}_{\text{old}}$ – $\pi_{\text{old}}$ ; thus the mixing between  $\text{SYM}_{\text{old}}$ – $\pi_{\text{old}}^*$  is stronger than between  $\text{SYM}_{\text{old}}$ – $\pi_{\text{old}}$ , and after all,  $\text{SYM}_{\text{old}}$  level is lowered. As a result, the final  $\text{SYM}_{\text{new}}$ –ASYM gap in **2b** is larger than its unperturbed value (increasing from 0.080 to 0.113 au).

On the other hand, **2c** has a large initial gap of 0.128 au, compared to 0.080 au in **2b**, due to a stronger spatial overlap between the two  $p_z(\text{B})$  orbitals. This gap (0.128 au) is decreased to 0.093 au after orbital interactions between  $\text{SYM}_{\text{old}}$  and both  $\pi_{\text{old}}$  and  $\pi_{\text{old}}^*$ . Unlike **2b**, in **2c**,  $\delta\epsilon$  (0.313 au) of  $\text{SYM}_{\text{old}}$ – $\pi_{\text{old}}^*$  is actually slightly larger than  $\delta\epsilon$  (0.307 au) of  $\text{SYM}_{\text{old}}$ – $\pi_{\text{old}}$ , meaning that the mixing between  $\text{SYM}_{\text{old}}$ – $\pi_{\text{old}}$  is slightly

stronger than between  $\text{SYM}_{\text{old}}-\pi^*_{\text{old}}$ . Therefore, the  $\text{SYM}_{\text{old}}$  level in **2c** is eventually raised and the  $\text{SYM}_{\text{new}}-\text{ASYM}$  gap becomes smaller (from 0.128 to 0.093 au).

It is noted that the much shorter bond distance between B–N (1.58 Å) in **2c** than B–P (1.92 Å) in **2b** means **2c** has a much stronger exchange interaction and thus larger matrix elements ( $V$ ). This means that, for a given  $\delta\epsilon$ , because  $\Delta$  ( $\sim V^2/\delta\epsilon$ ) is proportional to the square of matrix elements ( $V$ ) and inversely proportional to the energy gap ( $\delta\epsilon$ ), **2c** will generally have a greater mixing than **2b**. However, **2c** has a much smaller relative difference in  $\delta\epsilon$  (0.307 vs 0.313 au) for the two relevant mixings in Figure 2, causing a smaller relative shifting of  $\text{SYM}_{\text{old}}$ , as compared to **2b** (0.278 vs 0.145 au). As a consequence, the balance between  $V$  (which is greater in **2c**) and  $\delta\epsilon$  (for which a relative difference is greater in **2b**) makes  $\text{SYM}_{\text{old}}$  of **2b** and **2c** both shifted by almost the same extent overall (i.e.,  $\Delta = -0.033$  and  $+0.035$  au for **2b** and **2c**, respectively).

In summary, whereas  $\pi_{\text{old}}$  and  $\pi^*_{\text{old}}$  both interact with  $\text{SYM}_{\text{old}}$ , **2b** has relatively stronger mixing with  $\pi^*_{\text{old}}$  whereas **2c** has relatively stronger mixing with  $\pi_{\text{old}}$ . As a result, despite a longer B–B distance in **2b** than **2c**, **2b** has a larger final  $\text{SYM}_{\text{new}}-\text{ASYM}$  gap than **2c** and thus is less diradicaloid (consistent with the occupation numbers in Table 1).

Because the orbital interaction diagrams (Figure 2) for **2b** and **2c** represent only the relative strengths of different interactions (i.e.,  $\text{SYM}_{\text{old}}-\pi_{\text{old}}$  vs  $\text{SYM}_{\text{old}}-\pi^*_{\text{old}}$ ), to get some insight about the absolute strength of individual orbital mixing,  $\text{PH}_2$  and  $\text{NH}_2$  groups in **2b** and **2c** were replaced by SH (**2e**) and OH (**2f**) groups, respectively. Only the  $D_{2h}$  potential energy surface (planar geometry) is considered for **2e** and **2f**. In planar **2e** and **2f**, there is no analogue of the (empty)  $\pi^*_{\text{old}}$  orbital in **2b** or **2c** that has the same symmetry as  $\text{SYM}_{\text{old}}$ , and only the symmetric combination ( $\pi_{\text{old}}$ ) of (filled) atomic  $p_z$  orbitals centered on S (or O) has the proper symmetry to be mixed with  $\text{SYM}_{\text{old}}$ , as can be seen in Figure 3. Thus, this particular substitution guarantees that the splitting of  $\text{SYM}_{\text{old}}$  is now only a result of a mixing with the out-of-phase (relative to  $\text{SYM}_{\text{old}}$ ) symmetric combination  $\pi_{\text{old}}$ , unlike **2b** or **2c** (Figure 3).

**2e** and **2f** with  $D_{2h}$  symmetry were optimized with the PP/6-31G(d) method, and single point RB3LYP/6-31G(d) calculations were performed to obtain  $\text{SYM}_{\text{old}}$  and  $\text{ASYM}$  orbital energies using  $^{\ominus}\text{BH}_2-$   $^{\ominus}\text{BH}_2^*$  models with optimized B–B distances.<sup>24</sup> The PP optimized B–B distance in **2e** is 2.84 Å and that in **2f** is 2.25 Å. This result is not surprising because sulfur is bigger than oxygen and thus **2f** is structurally more compact than **2e**. For  $\pi_{\text{old}}$  orbital energies,  $^{\bullet}\text{SH}$  and  $^{\bullet}\text{OH}$  radicals were used. The resulting orbital interaction diagrams for **2e** and **2f** are summarized in Figure 3.

There are two conclusions that can be drawn from these model compounds, **2e** and **2f**. First, in both cases, the degree of mixing between  $\text{SYM}_{\text{old}}$  and  $\pi_{\text{old}}$  is so substantial that it even alters the ordering of orbitals. In other words, after the orbital interaction (Figure 3),  $\text{ASYM}$  becomes a HOMO despite the fact that there is a nodal plane between the two boron  $p_z(\text{B})$  orbitals in  $\text{ASYM}$ . Second, the structurally more compact **2f** ( $\Delta \sim 0.192$  au) has a stronger mixing or splitting than **2e** ( $\Delta \sim 0.173$  au) with a longer B–B distance, even though  $\delta\epsilon$  for **2f** is larger (0.190 au) than  $\delta\epsilon$  for **2e** (0.170 au). This result indicates that matrix elements ( $V$ ) that are strongly related to spatial overlap between MOs that are mixing are more important than their energy differences ( $\delta\epsilon$ ) in determining the splitting ( $\Delta$ ). This is consistent with second-order perturbation theory, because  $\Delta$  ( $\sim V^2/\delta\epsilon$ ) is inversely proportional to  $\delta\epsilon$  but proportional to the *square* of matrix elements ( $V$ ). As a consequence, **2f**

becomes more diradicaloid than **2e** despite a larger initial  $\text{SYM}_{\text{old}}-\text{ASYM}$  gap.

The final HOMO–LUMO gaps (or equivalently  $\text{ASYM}-\text{SYM}_{\text{new}}$  gaps in terms of the notations in Figure 3) in **2e** and **2f** are also in excellent agreement with the PP occupation numbers. The LUMO occupation number of **2e** is 0.316 whereas **2f** has 0.533. A smaller HOMO–LUMO gap consistently shows more diradical character for **2b**, **2c**, **2e**, and **2f**. The decreasing order of HOMO–LUMO gaps (in hartrees) is **2b** (0.113 au), **2e** (0.105 au), **2c** (0.093 au), and **2f** (0.085 au), whereas the increasing order of diradical character (in LUMO occupation number) is **2b** (0.221), **2e** (0.316), **2c** (0.437), and **2f** (0.533).

## Conclusions

(1) The extent of diradical character of **2d**, a recently reported “localized singlet diradical that is indefinitely stable at room temperature”, was assessed using perfect pairing orbital occupation numbers against a variety of related compounds and existing diradicals. The LUMO occupation number of **2d** is 0.169, which is far smaller than the theoretical value of 1 for a “pure” diradical and most other well-known organic diradicals. The implication of this result is that **2d** is indefinitely stable in a singlet state at room temperature due to its dominant bonding character (and remaining moderate extent of diradical character) between the two radical sites. The fact that broken symmetry spin-unrestricted B3LYP calculations of  $\langle S^2 \rangle_{\text{UB3LYP}}$  for the same compounds also show a similar trend as the PP occupation numbers supports the empirical use of  $\langle S^2 \rangle_{\text{UB3LYP}}$  as a quick way of estimating the extent of diradical character.

(2) We discovered that, unlike usual diradical systems, **2c** with a shorter B–B distance (2.04 Å) is more diradicaloid than **2b** with a longer B–B distance (2.60 Å). Together with the surprising stability of **2d** (and **2b**), this suggests that electronic interactions with substituents are controlling the extent of diradical character.

(3) A qualitative understanding of the factors determining the extent of diradical character of **2b** relative to **2c** was then obtained using standard orbital interaction arguments. Three factors played a role: (i) the initial gap between in-phase ( $\text{SYM}$ ) and out-of-phase ( $\text{ASYM}$ ) combinations of boron  $p_z$  orbitals, as determined by the B–B distance. This initial gap is then modified by (ii) the stabilization of the in-phase ( $\text{SYM}$ ) orbital due to coupling with higher energy antibonding orbitals ( $\pi^*$ ) of appropriate symmetry from the  $\text{YH}_2$  ( $\text{Y} = \text{P}, \text{N}$ ) groups, and (iii) the destabilization of the in-phase ( $\text{SYM}$ ) orbital due to coupling with lower energy bonding orbitals ( $\pi$ ) of appropriate symmetry from the  $\text{YH}_2$  groups, or  $\text{ZH}$  ( $\text{Z} = \text{S}, \text{O}$ ).

(4) For model compounds **2e** and **2f** (Figure 3), only effects (i) and (iii) are operative, and the destabilization (effect (iii)) is so strong that the out-of-phase ( $\text{ASYM}$ ) combination of boron  $p_z$  orbitals is left lower in energy than the in-phase combination.

(5) For **2c** and **2b** (Figure 2), stabilizing effect (ii) restores the in-phase ( $\text{SYM}$ ) orbital to lower energy than the out-of-phase. This effect is stronger in **2b**, leading to a larger gap, lower diradicaloid character, and greater stability.

(6) A deeper understanding of how the extent of diradical character changes as a result of substitution to stabilize (or destabilize) the singlet diradical is of great potential importance, because this will help organic chemists synthesize more stable singlet diradicals with controllable amounts of diradical character. Further theoretical studies should be directed toward this goal.

**Acknowledgment.** This work was supported by grant CHE-9981997 from the National Science Foundation. M.H.G. is on

appointment as a Miller Research Professor in the Miller Institute for Basic Research in Science. We thank Professor Borden at University of Washington for his invaluable comments on this paper.

## References and Notes

- (1) (a) Salem, L.; Rowland, C. *Angew. Chem., Int. Ed. Engl.* **1972**, *11*, 92–111. (b) Rajca, A. *Chem. Rev.* **1994**, *94*, 871–893. (c) Flynn, C.; Michl, J. *J. Am. Chem. Soc.* **1974**, *96*, 3280–3288. (d) Dohnert, D.; Koutecky, J. *J. Am. Chem. Soc.* **1980**, *102*, 1789–1796. (e) Bonacic-Koutecky, V.; Koutecky, J.; Michl, J. *Angew. Chem., Int. Ed. Engl.* **1987**, *26*, 170–189.
- (2) (a) *Diradicals*; Borden, W. T., Ed.; Wiley-Interscience: New York, 1982. (b) *Encyclopedia of Computational Chemistry*; Schleyer, P. v., Ed.; Wiley-Interscience: New York, 1998; pp 708–722. (c) Borden, W. T.; Iwamura, H.; Berson, J. A. *Acc. Chem. Res.* **1994**, *27*, 109–116. (d) Pedersen, S.; Herek, J. L.; Zewail, A. H. *Science* **1994**, *266*, 1359. (e) Berson, J. A. *Science* **1994**, *266*, 1338. (f) Zewail, A. H. *Angew. Chem., Int. Ed. Engl.* **2000**, *29*, 2587.
- (3) (a) Jain, R.; Sponsler, M. B.; Combs, F. D.; Dougherty, D. A. *J. Am. Chem. Soc.* **1988**, *110*, 1356–1366. (b) Berson, J. A. *Acc. Chem. Res.* **1997**, *30*, 238–244.
- (4) (a) Buchwalter, S. L.; Closs, G. L. *J. Am. Chem. Soc.* **1975**, *97*, 3857. (b) Buchwalter, S. L.; Closs, G. L. *J. Am. Chem. Soc.* **1979**, *101*, 4688–4694.
- (5) (a) Conrad, M. P.; Pitzer, R. M.; Schaefer, H. F. *J. Am. Chem. Soc.* **1979**, *101*, 2245. (b) Sherrill, C. D.; Seidl, E. T.; Schaefer, H. F. *J. Phys. Chem.* **1992**, *96*, 3712–3716.
- (6) *Diradicals*; Borden, W. T., Ed.; Wiley-Interscience: New York, 1982 (see pp 283–321 for *Intersystem crossing in diradicals and radical pairs*).
- (7) (a) Xu, J. D.; Hrovat, D. A.; Borden, W. T. *J. Am. Chem. Soc.* **1994**, *116*, 5425–5427. (b) Adam, W.; Borden, W. T.; Burda, C.; Foster, H.; Heidenfelder, T.; Heubes, M.; Hrovat, D. A.; Kita, F.; Lewis, S. B.; Scheutzwang, D.; Wirz, J. *J. Am. Chem. Soc.* **1998**, *120*, 953–954. (c) Abe, M.; Adam, W.; Heidenfelder, T.; Nau, W. M.; Zhang, X. *J. Am. Chem. Soc.* **2000**, *122*, 2019–2026. (d) Abe, M.; Adam, W.; Hara, M.; Hattori, M.; Majima, T.; Nojima, M.; Tachibana, K.; Tojo, S. *J. Am. Chem. Soc.* **2002**, In press. (e) Because **1b** was calculated to be a transition state species for a ring conversion, additional phenyl substitution was needed in experiment to make a more stable singlet diradical (See refs 7a,b). (f) Adam, W.; Frohlich, L.; Nau, W. M.; Wirz, J. *J. Am. Chem. Soc.* **1993**, *115*, 9824–9825. (g) Bush, L. C.; Heath, R. B.; Berson, J. A. *J. Am. Chem. Soc.* **1993**, *115*, 9830–9831. (h) Bush, L. C.; Heath, R. B.; Feng, X. W.; Wang, P. A.; Maksimovic, L.; Song, A. I.; Chung, W. S.; Berinstain, A. B.; Scaiano, J. C.; Berson, J. A. *J. Am. Chem. Soc.* **1997**, *119*, 1406–1415.
- (8) Scheschkewitz, D.; Amii, H.; Gornitzka, H.; Schoeller, W. W.; Bourissou, D.; Bertrand, G. *Science* **2002**, *295*, 1880–1881.
- (9) (a) Cullen, J. *Chem. Phys.* **1996**, *202*, 217. (b) Voorhis, T. V.; Head-Gordon, M. *J. Chem. Phys.* **2000**, *112*, 5633–5638. (c) Voorhis, T. V.; Head-Gordon, M. *J. Chem. Phys.* **2002**, *117*, 9190–9201. (d) Hariharan, P. C.; Pople, J. A. *Theor. Chim. Acta* **1973**, *28*, 212. (e) Kong, J.; White, C. A.; Krylov, A. I.; Sherrill, D.; Adamson, R. D.; Furlani, T. R.; Lee, M. S.; Lee, A. M.; Gwaltney, S. R.; Adams, T. R.; Ochsenfeld, C.; Gilbert, A. T. B.; Kedziora, G. S.; Rassolov, V. A.; Maurice, D. R.; Nair, N.; Shao, Y. H.; Besley, N. A.; Maslen, P. E.; Dombroski, J. P.; Daschel, H.; Zhang, W. M.; Korambath, P. P.; Baker, J.; Byrd, E. F. C.; Van Voorhis, T.; Oumi, M.; Hirata, S.; Hsu, C. P.; Ishikawa, N.; Florian, J.; Warshel, A.; Johnson, B. G.; Gill, P. M. W.; Head-Gordon, M.; Pople, J. A. *J. Comput. Chem.* **2000**, *21*, 1532–1548.
- (10) Nguyen, K. A.; Gordon, M. S.; Boatz, J. A. *J. Am. Chem. Soc.* **1994**, *116*, 9241–9249.
- (11) (a) Krylov, A. *Chem. Phys. Lett.* **2001**, *338*, 375–384. (b) Krylov, A. *Chem. Phys. Lett.* **2001**, *350*, 522–530. (c) Krylov, A. I.; Sherrill, C. D. *J. Chem. Phys.* **2002**, *116*, 3194–3203. (d) Shao, Y.; Head-Gordon, M.; Krylov, A. *J. Chem. Phys.* **2003**, *118*, 4807–4818. (e) *Quantum Theory of Many-Particle Systems*; Fetter, A. L., Walecka, J. D., Eds.; McGraw-Hill: New York, 1971. (f) Hirata, S.; Head-Gordon, M. *Chem. Phys. Lett.* **1999**, *302*, 375–382. (g) Hirata, S.; Head-Gordon, M. *Chem. Phys. Lett.* **1999**, *314*, 291–299. (h) Single point SF-TDDFT/TDA calculations with a bigger basis, 6-311++G(d, p), on the SF-TDDFT/TDA/6-31G(d) optimized geometries yielded a similar result, a singlet–triplet separation of –25.2 kcal/mol.
- (12) Hamers, R. J.; Wang, Y. *Chem. Rev.* **1996**, *96*, 1261–1290.
- (13) (a) Shoemaker, J.; Burggraf, J. W.; Gordon, M. S. *J. Chem. Phys.* **2000**, *112*, 2994. (b) Jung, Y.; Akinaga, Y.; Jordan, K. D.; Gordon, M. S. *Theo. Chem. Acc.*, in press.
- (14) (a) Hoffman, R. *J. Am. Chem. Soc.* **1968**, *90*, 1475. (b) Hoffman, R. *Acc. Chem. Res.* **1971**, *4*, 1–9. (c) Dougherty, D. A. *Acc. Chem. Res.* **1991**, *24*, 88–94. (d) Getty, S. J.; Hrovat, D. A.; Borden, W. T. *J. Am. Chem. Soc.* **1994**, *116*, 1512–1527. (e) Schoeller, W. W.; Dabisch, T.; Busch, T. *Inorg. Chem.* **1987**, *26*, 4383–4389.
- (15) Wolf, S. A.; Awaschalom, D. D.; Buhman, R. A.; Daughton, J. M.; Molnar, S. v.; Roukes, M. L.; Chtchelkanova, A. Y.; Treger, D. M. *Science* **2001**, *294*, 1488–1495 (review article).
- (16) Natural orbitals are the ones that diagonalize the one particle density matrix, and then the natural orbital occupation numbers are its eigenvalues. See *Modern Quantum Chemistry: Introduction to Advanced Electronic Structure Theory* by Attila Szabo and Neil S. Ostlund.
- (17) Schmidt, M. W.; Gordon, M. S. *Annu. Rev. Phys. Chem.* **1998**, *49*, 233–266.
- (18) (a) Staroverov, V. N.; Davidson, E. R. *J. Am. Chem. Soc.* **2000**, *122*, 186–187. (b) Hrovat, D. A.; Duncan, J. A.; Borden, W. T. *J. Am. Chem. Soc.* **1999**, *121*, 169–175. (c) Head-Gordon, M. *Chem. Phys. Lett.* **2003**, *372*, 508–511.
- (19) Pople, A. J.; Gill, P. M. W.; Handy, N. C. *Intl. J. Quantum. Chem.* **1995**, *56*, 303–305.
- (20) (a) Seierstad, M.; Kinsinger, C. R.; Cramer, C. J. *Angew. Chem., Int. Ed. Engl.* **2002**, *41*, 3894–3896. (b) Jung, Y.; Head-Gordon, M. *ChemPhysChem* **2003**, *4*, 522–525.
- (21) Jung, Y.; Shao, Y.; Gordon, M. S.; Doren, D.; Head-Gordon, M. Submitted to *J. Chem. Phys.*
- (22) Seeger, R.; Pople, J. A. *J. Chem. Phys.* **1977**, *66*, 3045–3050.
- (23) Although  ${}^{\ominus}\text{PH}_4$  appears to be a better model than  $\text{PH}_3$  for estimating unperturbed orbital energies in the sense that  ${}^{\ominus}\text{PH}_4$  has the same formal charge on P as **2b** and also a similar  $\sigma$  framework, very negative absolute orbital energies of cationic  ${}^{\oplus}\text{PH}_4$  (for example, –0.22 au for the P–H antibond) as compared to **2b** make its use irrelevant in constructing an orbital mixing diagram. It is also possible to consider neutral  ${}^{\ominus}\text{BH}_2$ - ${}^{\oplus}\text{PH}_3$  species, which have the same formal charge on P and similar  $\sigma$  framework as **2b**, but this model already has some orbital mixing (with  $\text{BH}_2$  group) in it, and thus is inappropriate for unperturbed orbital energies. The same holds for  $\text{NH}_3$  fragment.
- (24) For  ${}^{\ominus}\text{BH}_2$ - ${}^{\oplus}\text{BH}_2^*$  with B–B distance of 2.602 Å (which is the PP optimized distance for **2b**), there is a long  $\sigma$  bond between borons ( $\text{SYM}_{\text{old}}-1$ ), and one remaining valence electron from each boron forms a weakly overlapping  $\pi$  bond ( $\text{SYM}_{\text{old}}$ ). The initial  $\text{SYM}_{\text{old}}-\text{ASYM}$  gap of 0.080 au for **2b** in Figure 2 is the gap between this orbital ( $\text{SYM}_{\text{old}}$ ) and its correlating unoccupied antibonding orbital. The same holds for **2c**, **2e**, and **2f**.  ${}^{\ominus}\text{BH}_2$ - ${}^{\oplus}\text{BH}_2^*$  also has the same formal charge on B as **2b-f**.